Capacitive Wireless Power Transfer with Multiple Transmitters: Efficiency Optimization

Ben Minnaert [1,*] ![ORCID], **Alessandra Costanzo** [2] ![ORCID], **Giuseppina Monti** [3] **and and Mauro Mongiardo** [4]

[1] Department of Industrial Science and Technology, Odisee University College of Applied Sciences, 9000 Ghent, Belgium

[2] Department of Electrical, Electronic and Information Engineering Guglielmo Marconi, University of Bologna, 40126 Bologna, Italy; alessandra.costanzo@unibo.it

[3] Department of Engineering for Innovation, University of Salento, 73100 Lecce, Italy; giuseppina.monti@unisalento.it

[4] Department of Engineering, University of Perugia, 06123 Perugia, Italy; mauro.mongiardo@unipg.it

[*] Correspondence: ben.minnaert@odisee.be

![check for updates]

Abstract: Wireless power transfer with multiple transmitters can have several advantages, including more robustness against misalignment and extending the mobility and range of the receiver(s). In this work, the efficiency maximization problem is analytically solved for a capacitive wireless power transfer system with multiple coupled transmitters and a single receiver. It is found that the system efficiency can be increased by adding more transmitters. Moreover, it is proven that the cross-coupling between the transmitters can be eliminated by adding shunt susceptances at the input ports. Optimal values for the input currents and receiver load are determined to achieve maximum efficiency. As well the optimal load, the optimal input currents and the maximum efficiency are independent on the cross-coupling. By impedance-matching the internal conductances of the generators, the maximum-efficiency solution also becomes the one that provides the maximum output power. Finally, by expressing each transmitter–receiver link with its kQ-product, the maximum system efficiency can be calculated. The analytical results are verified by circuital simulation.

Keywords: capacitive wireless power transfer; resonance; wireless power transfer; power-transfer efficiency; multiports; multiple-input single-output

1. Introduction

Near-field wireless power transfer (WPT) represents a promising solution for wirelessly providing power to electronic devices. Two main technologies exist: inductive and capacitive WPT, based on resonant magnetic or electric coupling, respectively. The simplest setup consists of two resonators: a transmitting resonator, powered by an input supply, which transfers power wirelessly to a receiving resonator connected to the load (SISO: single-input single-output).

For certain applications, WPT from multiple transmitters to a single receiver (MISO: multiple-input single-output) can be beneficial compared to the single-transmitter configuration:

- First, multiple transmitters targeting a single receiver results in a certain robustness against misalignment or mispositioning of the receiver. This extends the mobility of the receiver. If, for example, multiple transmitters are present in a planar configuration, the power transfer can be realized for a wide possibility of planar receiver positions.
- Second, the above implies that the use of multiple transmitters can extend the range of the wireless power transfer.

- A decentralization of the transmitters can possibly facilitate high-power energy transfer by applying multiple cheaper low-power input supplies.
- Multiple transmitters make the WPT system less vulnerable to foreign blocking objects.
- Last but not least, as will be shown in this work, multiple transmitters allow for a higher system efficiency for given coupling coefficients since they allow for a higher degree of freedom for the power input distribution.

In this work, focus will lie on capacitive power transfer (CPT), which utilizes a high-frequency electric field as a medium to transfer energy wirelessly. Main advantages compared to inductive WPT are low-weight and cost, a minimal eddy-current loss, and a larger robustness against misalignment. A typical CPT coupler consists of four metal plates: two plates at the transmitter side, and two at the receiver side, resulting in a return path for the current [1]. CPT has been demonstrated in low-power applications such as portable electronics [2,3], integrated circuits [4], drones [5], and biomedical devices [6,7]. However, also at higher power levels, up to several kW [8], CPT can be applied—e.g., in automatic guided vehicles [9] and electric vehicles [10–12].

Maximizing the efficiency of an *inductive* WPT system with multiple transmitters has already been solved, e.g., [13–18]. Additionally, for the general WPT system, this problem has been solved by reducing the entire system to an impedance matrix of a multiport network [19–21]. However, this methodology loses the internal structure of the WPT system, e.g., the coupling strengths between transmitters and receiver. Moreover, a CPT system can be more easily described by its admittance matrix instead of its impedance matrix.

Efficiency maximization for CPT was already solved for a single transmitter with multiple receivers (SIMO: single-input multiple-output) [22,23], but to date, an analysis specifically for a CPT system with multiple (coupled) transmitters (MISO) is lacking.

In this work, a CPT transfer system with *any* number of transmitters and a single receiver is considered. Varying the receiver's loads (e.g., via impedance matching) and/or the input currents results in different values for the power-transfer efficiency (also called power gain) of the CPT system. In this work, the load and input currents that maximize the power-transfer efficiency are determined while taking into account, among others, the coupling strengths between transmitters and receiver. More specifically, the contributions are the following:

- After constructing the general CPT system with N transmitters and a single receiver (Section 2), the input power, output power, and efficiency as functions of the characteristics of the network are determined (Section 3).
- The optimal current–voltage relationships at the transmitter and receiver ports are calculated (Section 4). From these relationships, closed-form expressions for the optimal load, input current ratios, and the maximum efficiency are analytically determined (Section 4).
- By matching the internal shunt admittance of the generators to the system, the maximum-efficiency solution coincides with the configuration that maximizes the output power (Section 4).
- It is shown that the cross-coupling between the transmitters does not influence the value of the maximum efficiency or optimal load: by including a reactive part at the transmitter side, the impact of cross-coupling can be neutralized. Moreover, the efficiency of the CPT system can be increased by adding extra transmitters (Section 5).
- It is demonstrated that the maximum efficiency of the multiple transmitter system can be estimated by measuring the individual transmitter–receiver links (Section 5).
- Finally, the analytical solution is demonstrated on an example equivalent circuit of a CPT system. The results are verified by numerical circuit simulation for a system with three transmitters and a single receiver (Section 6).

2. Problem Description

Figure 1 depicts a CPT system with N transmitters (on the bottom, subscripts 1 to N) and a single receiver (on top, subscript 0). The transmitters are powered by a power supply control circuit. Each transmitter can operate at a different voltage and phase, but the operating angular frequency ω_0 is the same for all transmitters. The resistive and reactive components within each transmitter are described by the conductances g_{nn} and susceptances b_{nn} ($n = 1, \ldots, N$), respectively. In the remainder of this work, the subscript n always counts from 1 to N.
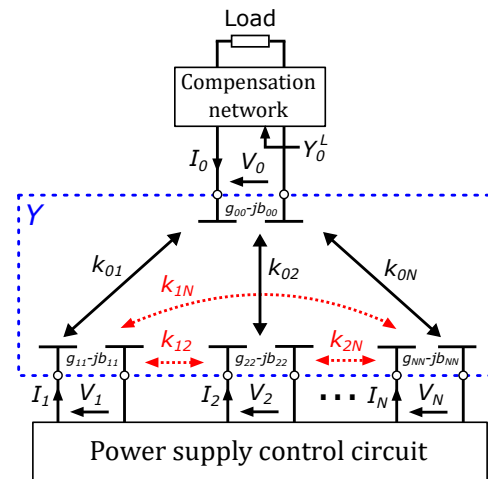

Figure 1. A general capacitive wireless power transfer system with N transmitters (bottom) and a single receiver (top). The (desired) electric couplings between transmitters and receiver are depicted by the full arrows. The undesired cross-couplings between the transmitters themselves are indicated by the dashed arrows.

Energy is transferred wirelessly to the load of the receiver, represented by the admittance Y_0^L (including a possible compensation circuit). The conductance g_{00} and susceptance b_{00} correspond to the resistive and reactive part of the receiving resonator, respectively.

The strength of the electric coupling between each transmitter and the receiver is given by the coupling factor k_{0n}, a dimensionless number which can vary from zero (no coupling) to unity (maximum coupling). In a practical CPT system, the electric coupling between the transmitters and receiver is desired to realize wireless power transmission. However, an undesired (nonzero) electric cross-coupling can be present between the transmitters themselves, represented by k_{nm} ($n, m = 1, \ldots, N; n \neq m$). The coupling factor is defined as [24,25]

$$k_{ij} = \frac{C_{ij}}{\sqrt{C_i C_j}}, \tag{1}$$

for $i, j = 0, \ldots, N; i \neq j$, where C_n is the transmitter capacitance of the n-th transmitter, C_0 is the receiver capacitance, and C_{ij} is the mutual capacitance, corresponding to the electric coupling. Note that C_0 and C_n do not correspond to the capacitance between the physical transmitter and receiver plate, but to an equivalent circuit representation of electric coupling [25]. The measurement procedure to determine the value of these capacitances is described in [24].

The CPT system can be considered as a multiport with N input ports (the N transmitters) and one output port (the receiver). The multiport is indicated by the dashed rectangle in Figure 1. Notice that this $(N + 1)$-port network is linear and reciprocal due to the passive components it is constructed from. The currents through and voltages at the $(N + 1)$ ports are given by the peak current phasors I_j and peak voltage phasors V_j, as defined in Figure 1 ($j = 0, \ldots, N$).

The problem description is the following: given the network of Figure 1 (with given and fixed values for the components of the CPT network and coupling factors), determine the values of the load admittance Y_0^L and input currents I_n that maximize the power-transfer efficiency η. The problem can be reduced to finding the current and voltage phasors at the ports, corresponding to the optimal efficiency configuration. Therefore, any remote electronics external to the wireless link (e.g., rectifiers, matching networks, actual passive loads,...) can be ignored, since it can be taken into account once the optimal current–voltage relationship at the ports are determined.

3. Power and Efficiency of the CPT System

First, the (normalized) admittance matrix, input power, output power, and efficiency will be expressed as functions of the characteristics of the network. The efficiency is not yet maximized in this section.

3.1. Admittance Matrix

The CPT system can be fully characterized by its admittance matrix Y. The admittance matrix Y describes the relation between the port currents and port voltages:

$$I = Y \cdot V, \tag{2}$$

with the $(N + 1) \times 1$ matrices V and I defined as

$$V = \begin{bmatrix} V_1 \\ V_2 \\ \vdots \\ V_N \\ V_0 \end{bmatrix}, I = \begin{bmatrix} I_1 \\ I_2 \\ \vdots \\ I_N \\ I_0 \end{bmatrix}. \tag{3}$$

The admittance matrix Y of the CPT system can be written as [25]

$$Y = \begin{bmatrix} g_{11} - jb_{11} & -jb_{12} & \cdots & -jb_{1N} & -jb_{10} \\ -jb_{21} & g_{22} - jb_{22} & \cdots & -jb_{2N} & -jb_{20} \\ \vdots & \vdots & \ddots & \vdots & \vdots \\ -jb_{N1} & -jb_{N2} & \cdots & g_{NN} - jb_{NN} & -jb_{N0} \\ -jb_{01} & -jb_{02} & \cdots & -jb_{0N} & g_{00} - jb_{00} \end{bmatrix}, \tag{4}$$

with $b_{ij} = \omega_0 C_{ij}$, $(i, j = 0, \ldots, N; i \neq j)$. Since the network is reciprocal, Y is symmetric: $b_{ij} = b_{ji}$. In practical applications, the admittance matrix Y can be measured. Note that each transmitter and the receiver have a self-susceptance expressed by $-b_{jj}$.

A normalization matrix n is defined:

$$n = \begin{bmatrix} \frac{1}{\sqrt{\omega_0 C_1}} & \cdots & 0 & 0 \\ \vdots & \ddots & \vdots & \vdots \\ 0 & \cdots & \frac{1}{\sqrt{\omega_0 C_N}} & 0 \\ 0 & \cdots & 0 & \frac{1}{\sqrt{\omega_0 C_0}} \end{bmatrix}, \tag{5}$$

in order to normalize the admittance matrix:

$$
\boldsymbol{y} = \boldsymbol{n} \cdot \boldsymbol{Y} \cdot \boldsymbol{n} =
\begin{bmatrix}
\frac{1}{Q_1} - jk_{11} & \cdots & -jk_{1N} & -jk_{10} \\
\vdots & \ddots & \vdots & \vdots \\
-jk_{N1} & \cdots & \frac{1}{Q_N} - jk_{NN} & -jk_{N0} \\
-jk_{01} & \cdots & -jk_{0N} & \frac{1}{Q_0} - jk_{00}
\end{bmatrix},
\tag{6}
$$

with quality factor Q_i of the coupled resonators ($i, j = 0, \ldots, N$):

$$
Q_i = \frac{\omega_0 C_i}{g_{ii}}
\tag{7}
$$

and

$$
k_{ij} = \frac{b_{ij}}{\omega_0 \sqrt{C_i C_j}}.
\tag{8}
$$

For $i \neq j$, the parameter k_{ij} corresponds to the coupling factor between circuits i and j.
The voltages and currents are normalized as follows:

$$
\boldsymbol{i} = \boldsymbol{n} \cdot \boldsymbol{I},
\tag{9}
$$

$$
\boldsymbol{v} = \boldsymbol{n}^{-1} \cdot \boldsymbol{V}.
\tag{10}
$$

The normalized current–voltage relationship is thus given by

$$
\boldsymbol{i} = \boldsymbol{y} \cdot \boldsymbol{v}.
\tag{11}
$$

The real and imaginary parts of the (normalized) current and voltage phasors can be explicitly written out: $i_n = i_n^{re} + ji_n^{im}$ and $v_n = v_n^{re} + jv_n^{im}$. Without loss of generality, we choose v_0 as the reference phasor, i.e., $v_0^{re} = v_0$, $v_0^{im} = 0$.

3.2. Input Power

The input power P_n ($n = 1, \ldots, N$) for the n-th transmitter system is given by

$$
P_n = \frac{1}{2} \Re(v_n i_n^*),
\tag{12}
$$

where i_n^* is the complex conjugate of i_n, and $\Re(v_n i_n^*)$ is the real part of $v_n i_n^*$. This result for P_n is

$$
P_n = \frac{1}{2}(v_n^{re} i_n^{re} + v_n^{im} i_n^{im}).
\tag{13}
$$

The total input power P_{in} of the entire CPT system is

$$
P_{in} = \sum_{n=1}^{N} P_n.
\tag{14}
$$

Substituting the currents from Equation (11) into the above equation results in the total input power P_{in}:

$$
P_{in} = \frac{1}{2} \sum_{n=1}^{N} \frac{1}{Q_n} [(v_n^{re})^2 + (v_n^{im})^2] + \frac{1}{2} \sum_{n=1}^{N} k_{n0} v_0 v_n^{im}.
\tag{15}
$$

The input power P_{in} is expressed as function of the parameters of the network and the port voltages.

3.3. Output Power

Analogously, the output power can be determined as a function of the network variables and port voltages.

Applying the passive sign convention, the output power P_{out} can be written as

$$P_{out} = -\frac{1}{2}\Re(v_0 i_0^*) = -\frac{1}{2}v_0 i_0^{re}. \tag{16}$$

Substituting the currents from Equation (11) into the above equation, the normalized output power P_{out} is determined:

$$P_{out} = -\frac{1}{2Q_0}v_0^2 - \frac{1}{2}v_0\sum_{n=1}^{N}k_{0n}v_n^{im}. \tag{17}$$

3.4. Efficiency

The power-transfer efficiency η or power gain of the CPT system is defined as

$$\eta = \frac{P_{out}}{P_{in}}, \tag{18}$$

with the expressions for P_{in} and P_{out} given by Equations (15) and (17). Hence, η is written as a function of the parameters of the circuit and the port voltages.

4. Maximum-Efficiency Solution

In the previous section, the general expressions for input power, output power and efficiency were found. Now, the configuration at maximum power-transfer efficiency will be considered. The notation η_{max} is applied in this section to indicate that the power-transfer efficiency equals its maximum attainable value.

4.1. First-Order Necessary Condition

To find the output voltages at the maximum system efficiency configuration, the first-order necessary condition is applied to generate a system of $2N$ equations [20,26]:

$$\frac{\partial \eta}{\partial v_n^{re}} = 0, \tag{19}$$

$$\frac{\partial \eta}{\partial v_n^{im}} = 0. \tag{20}$$

The optimal input voltages v_n are the solution of the above system. Unfortunately, solving the system directly is not straightforward. First, the quotient rule for derivatives is applied. With Equation (18), the system becomes

$$P_{in}\frac{\partial P_{out}}{\partial v_n^{re}} - P_{out}\frac{\partial P_{in}}{\partial v_n^{re}} = 0, \tag{21}$$

$$P_{in}\frac{\partial P_{out}}{\partial v_n^{im}} - P_{out}\frac{\partial P_{in}}{\partial v_n^{im}} = 0. \tag{22}$$

Substituting the derivatives of Equations (15) and (17) to v_n^{re} and v_n^{im} into the system Equations (21) and (22), and taking into account Equation (18), the solution for the optimal normalized input voltages $v_n^{opt} = v_n^{re,opt} + jv_n^{im,opt}$ at each input port is found.

$$v_n^{re,opt} = 0, \tag{23}$$

$$v_n^{im,opt} = \frac{k_{0n} Q_n (\eta_{max} - 1)}{2\eta_{max}} v_0. \tag{24}$$

If the values of the normalized input port voltages v_n ($n = 1, \dots, N$) equal Equations (23) and (24), the maximum attainable efficiency η_{max} is reached. It is important to note that the voltages here are not only expressed as a function of the parameters of the circuit network (which are known and fixed) and the reference output voltage v_0, but also of the maximum efficiency η_{max}, which is (for now) an unknown value. In Section 4.3, the value of η_{max} will be determined.

4.2. Optimal Input and Output Power

By substituting Equations (23) and (24) into Equations (15) and (17), the input power P_{in}^{opt} and output power P_{out}^{opt} at the maximum efficiency configuration are determined:

$$P_{in}^{opt} = \frac{v_0^2 (1 - \eta_{max}^2) \alpha_N^2}{8 Q_0 \eta_{max}^2}, \tag{25}$$

$$P_{out}^{opt} = -\frac{v_0^2}{2 Q_0} \left[1 + \frac{(\eta_{max} - 1) \alpha_N^2}{2 \eta_{max}} \right], \tag{26}$$

where the following notation is introduced

$$\alpha_N^2 = \sum_{n=1}^{N} \alpha_n^2, \tag{27}$$

with

$$\alpha_n = k_{0n} \sqrt{Q_0 Q_n}. \tag{28}$$

The parameter α_n is named *the extended kQ-product* of the link between the n-th transmitter and the receiver, analogous to [27–29]. The variable α_N is called the *system kQ-product*, a naming borrowed from [14,15,29]. The introduction of these variables seems artificial at this point, but will be further discussed in Section 5.

The value of η_{max} is still unknown and will be determined in the following subsection.

4.3. Maximum Efficiency

A quadratic equation in η_{max} is found by substituting Equations (25) and (26) in Equation (18):

$$\eta_{max}^2 - \left(2 + \frac{4}{\alpha_N^2} \right) \eta_{max} + 1 = 0. \tag{29}$$

In order to alleviate the notation, the symbol γ is introduced:

$$\gamma = \sqrt{1 + \alpha_N^2}. \tag{30}$$

The quadratic Equation (29) results in two solutions:

$$\eta_{max,1} = \frac{\gamma - 1}{\gamma + 1}, \tag{31}$$

and

$$\eta_{max,2} = \frac{\gamma + 1}{\gamma - 1}. \tag{32}$$

Equation (32) is physically not possible since $0 \le \eta_{max} \le 1$. The maximum attainable power-transfer efficiency η_{max} is therefore expressed by Equation (31).

The maximum efficiency η_{max} is now determined as a function of the characteristics of the circuit parameters only, which implies that the optimal input voltages Equations (23) and (24), input Equation (25), and also output power Equation (26) are expressed as functions of the circuit characteristics only.

For example, the optimal output and input power are given by

$$P_{out}^{opt} = \frac{\gamma}{2Q_0} v_0^2, \tag{33}$$

$$P_{in}^{opt} = \frac{P_{out}^{opt}}{\eta_{max}} = \frac{\gamma}{2Q_0} \frac{\gamma + 1}{\gamma - 1} v_0^2. \tag{34}$$

4.4. Optimal Input Voltages, Currents, and Admittances

Combining Equations (23), (24), and (31), the optimal normalized input voltages $v_n^{opt} = v_n^{re,opt} + j v_n^{im,opt}$ are found:

$$v_n^{re,opt} = 0, \tag{35}$$

$$v_n^{im,opt} = \frac{k_{0n} Q_n}{1 - \gamma} v_0. \tag{36}$$

From Equations (11), the optimal normalized input currents $i_n^{opt} = i_n^{re,opt} + j i_n^{im,opt}$ follow

$$i_n^{re,opt} = \frac{v_0}{1 - \gamma} \sum_{i=1}^{N} k_{0i} k_{in} Q_i, \tag{37}$$

$$i_n^{im,opt} = \frac{\gamma k_{0n}}{1 - \gamma} v_0. \tag{38}$$

The optimal normalized input admittance $y_n^{in,opt}$ at port n thus equals

$$y_n^{in,opt} = \frac{i_n^{opt}}{v_n^{opt}} = \frac{\gamma}{Q_n} - j \frac{1}{k_{0n} Q_n} \sum_{i=1}^{N} k_{0i} k_{in} Q_i. \tag{39}$$

From this equation, it can be concluded that the cross-coupling between the transmitters can be compensated by a normalized shunt inductance b_n^S equal to

$$b_n^S = \frac{1}{k_{0n} Q_{nn}} \sum_{i=1}^{N} k_{0i} k_{in} Q_{ii}, \tag{40}$$

or unnormalized

$$B_n^S = \frac{g_{nn}}{b_{0n}} \sum_{i=1}^{N} \frac{b_{0i} b_{in}}{g_{ii}}. \tag{41}$$

Equation (39) implies that the optimal input conditions can be obtained by a set of N independent current generators operating in maximum power-transfer conditions. The internal normalized shunt admittances of these generators are

$$y_n^S = (y_n^{in,opt})^* = \frac{\gamma}{Q_n} + j \frac{1}{k_{0n} Q_n} \sum_{i=1}^{N} k_{0i} k_{in} Q_i, \tag{42}$$

and their normalized currents are

$$i_n^S = i_n^{opt} + y_n^S v_n^{opt} = 2j k_{0n} \frac{\gamma}{1 - \gamma} v_0. \tag{43}$$

In this way, maximum power transfer from the generators to the network is achieved. At this point, the maximum-efficiency solution also becomes the one that provides the maximum output power.

The corresponding unnormalized values of the shunt admittances and currents of these generators are (Figure 2a)

$$Y_n^S = \gamma g_{nn} + j \frac{g_{nn}}{b_{0n}} \sum_{i=1}^{N} \frac{b_{0i} b_{in}}{g_{ii}}, \tag{44}$$

$$I_n^S = 2jb_{0n} \frac{\gamma}{1-\gamma} V_0. \tag{45}$$

Since v_0 was chosen as reference phasor, the condition for the input current sources can be practically achieved by imposing that the ratios of the input currents must satisfy

$$\frac{i_G^S}{k_{01}} = \frac{i_2^S}{k_{02}} = \dots = \frac{i_N^S}{k_{0N}} \tag{46}$$

or

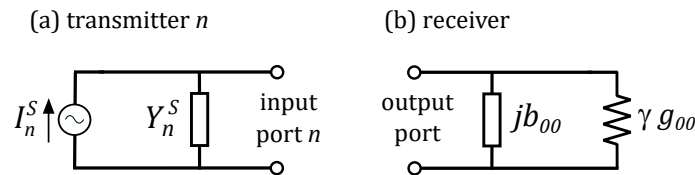$$\frac{I_1^S}{b_{01}} = \frac{I_2^S}{b_{02}} = \dots = \frac{I_N^S}{b_{0N}}. \tag{47}$$

(a) transmitter n　　　　　　　　　(b) receiver

Figure 2. Maximum-efficiency solution for (**a**) the transmitter ports with generator I_n^S and internal shunt admittance Y_n^S, and (**b**) the receiver port with the optimal load susceptance and load conductance.

4.5. Optimal Load Admittance

Finally, it is possible to determine the optimal load that realizes the maximum-efficiency solution. The optimal normalized load admittance is given by

$$y_0^{L,opt} = g_0^{L,opt} + jb_0^{L,opt} = -\frac{i_0^{opt}}{v_0^{opt}}, \tag{48}$$

where $g_0^{L,opt}$ and $b_0^{L,opt}$ are the optimal normalized load conductance and susceptance, respectively.

From Equation (11), it follows that

$$i_0^{re,opt} = \frac{v_0}{Q_0} + \sum_{n=1}^{N} k_{0n} v_n^{im,opt}, \tag{49}$$

$$i_0^{im,opt} = -k_{00} v_0 - \sum_{n=1}^{N} k_{0n} v_n^{re,opt}. \tag{50}$$

Substituting Equations (35) and (36) results into

$$i_0^{re,opt} = -\frac{\gamma}{Q_0} v_0, \tag{51}$$

$$i_0^{im,opt} = -k_{00} v_0, \tag{52}$$

which leads to the optimal normalized load conductance $g_0^{L,opt}$ and load susceptance $b_0^{L,opt}$ as functions of the parameters of the network:

$$g_0^{L,opt} = \frac{\gamma}{Q_0}, \tag{53}$$

$$b_0^{L,opt} = k_{00}. \tag{54}$$

The corresponding unnormalized values are (Figure 2b)

$$G_0^{L,opt} = \gamma g_{00}, \tag{55}$$

$$B_0^{L,opt} = b_{00}. \tag{56}$$

5. Discussion

In order to practically achieve the maximum attainable efficiency η_{max}, three conditions must be met simultaneously:

1. The value of the input current sources must satisfy Equation (47) (Figure 2a).
2. Shunt susceptances with value found in Equation (41) must be connected to each input port (Figure 2a).
3. The output load conductance and susceptance must equal Equations (55) and (56), respectively (Figure 2b).

Additionally, if the internal shunt admittances of the generators equal Equation (44), the maximum-efficiency solution also becomes the one that maximizes the output power.

The first condition indicates that, the higher the coupling between transmitter n and the receiver, the lower the necessary value of the current source for that transmitter. From Equations (35), (36), and (45), it follows that the phasors of the optimal current sources and optimal voltages of all input ports are orthogonal to the reference output voltage V_0.

Instead of applying current sources at each transmitter, one could also apply voltage sources for which the ratios must satisfy

$$V_1 : V_2 : \ldots : V_n = \frac{b_{01}}{g_{11}} : \frac{b_{02}}{g_{22}} : \ldots : \frac{b_{0n}}{g_{nn}}. \tag{57}$$

The optimal input voltages are in other words determined by the ratios between the transmitter–receiver coupling strength and the resistive losses of the transmitter.

The second condition, the insertion of shunt susceptances at the input port, is necessary to compensate for the cross-coupling between the transmitters. If no cross-coupling is present, no shunt susceptances have to be inserted, as can be seen by Equation (41).

Under the optimal conditions, the maximum efficiency η_{max} given by Equation (31) is reached. Notice that η_{max} is independent on the cross-coupling between the transmitters; the optimization of input voltages V_n^{opt} and load admittance $Y_0^{L,opt}$ eliminates the influence of the cross-coupling. Nevertheless, the presence of the shunt susceptances at the input ports is necessary for achieving η_{max} and to ensure that the optimal voltages V_n^{opt} are reached from the current sources I_n^S that supply the power for the CPT system.

The third condition refers to the terminating load. The optimal load conductance $G_0^{L,opt}$ of the receiver is proportionate to its parasitic conductance g_{00}. For high coupling ($\alpha_N \gg 1$) between the transmitters and receiver, the optimal conductance can be approximated by $G_0^{L,opt} = g_{00}\alpha_N$. The output load susceptance must equal Equation (56) and thus cancels out the self-susceptance of the receiver resonator.

The optimal terminating load admittance corresponds to the value found in scientific literature for a CPT system with a single transmitter ($N = 1$) coupled to a single receiver [30–32].

Notice that not only the maximum efficiency η_{max}, but also the optimal load and input current ratios are independent on the cross-coupling between the transmitters. For an uncoupled system, the maximum efficiency η_{max} and optimal load are the same as for a coupled system, since the shunt susceptances at the input ports compensate for the cross-coupling. This does not imply that the

efficiency is not influenced by cross-coupling for a *general* CPT system; it is the *maximum* efficiency that is invariant for cross-coupling for an *optimized* system towards efficiency.

The efficiency rises with higher couplings between transmitter and receiver, and lower conductances $g_{00}, g_{11}, \ldots, g_{NN}$ of the system.

It is not surprising that the maximum efficiency η_{max} is expressed as a function of a single variable; it is a general property of *any* reciprocal power transfer system that the efficiency can be stated as a function of a single scalar [28]. In the context of WPT with multiple transmitters and/or receivers, this variable is often called the system kQ-product [14,15,20,23]

From Equation (27), it can be concluded that the square of the system kQ-product equals the sum of the squares of the kQ products of each individual transmitter–receiver link. Determining the kQ product for each single transmitter–receiver pair thus results in a prediction for the entire system's power-transfer efficiency.

The higher the system kQ-product α_N, the higher the efficiency of the system, as can be seen by Equations (27), (28), and (31). The maximum efficiency η_{max} of the CPT system can thus be increased by adding more transmitters to the system, even if the transmitters themselves are coupled. Indeed, the cross-coupling between the transmitters can be compensated by the shunt susceptances B_n^S at the input ports. There is no optimal number of transmitters. The more transmitters, the higher the maximum attainable efficiency η_{max}.

6. Numerical Verification

In order to validate the theory, an example of CPT system with three transmitters ($N = 3$) and a single receiver is considered; it is assumed that there is a cross-coupling present between the transmitters themselves (Figure 3a). The parameters within the dashed rectangle are assumed to be given and fixed, including the coupling strengths. They can be represented by the admittance matrix $\mathbf{Y}$. In order to optimize the CPT system towards efficiency, it is possible to act on the value of the load $Y_0^L = G_0^L + jB_0^L$, the supply current sources I_G^S, and the input shunt susceptances B_n^S.
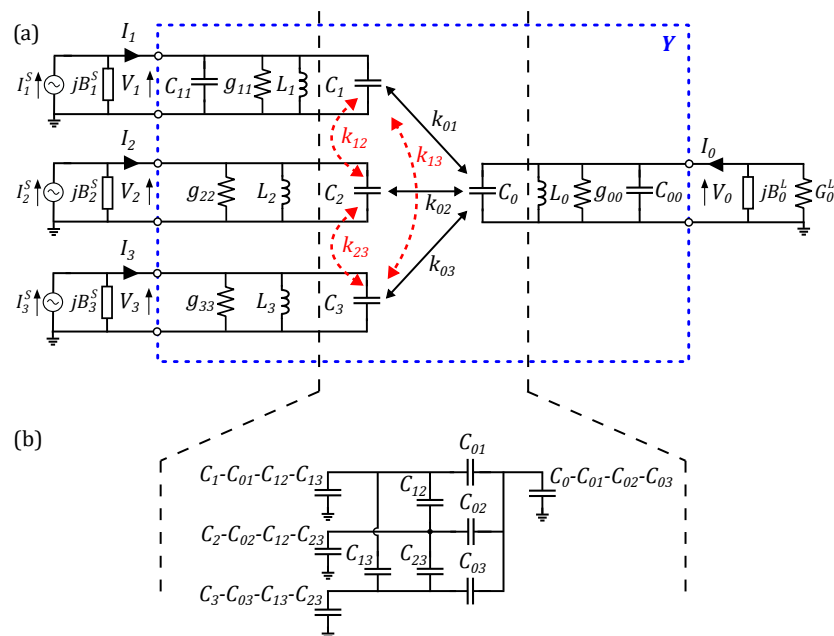

Figure 3. (**a**) Equivalent circuit of a capacitive wireless power transfer system with 3 transmitters (left) and a single receiver (right). The (desired) electric couplings between transmitters and receiver are depicted by the full arrows. The (undesired) cross-couplings between transmitters themselves are indicated by the dashed arrows. (**b**) Applied equivalent circuit for the simulation of the capacitive coupling.

The numerical values indicated in Table 1 are considered, the operating frequency is f_0=10 MHz. No specific design consideration is assumed; a range of different desired and undesired coupling factors (Table 2) were chosen to verify the analytical derivation. Further, it is assumed that the receiver and the first transmitter have a self-susceptance C_{00} and C_{11}, respectively.

Table 1. Given network simulation parameters for the analyzed numerical example.

Quantity	Value	Quantity	Value
f_0	10.0 MHz	I_1^S	100 mA
g_{00}	1.00 mS	C_0	350 pF
g_{11}	1.00 mS	C_1	350 pF
g_{22}	1.50 mS	C_2	300 pF
g_{33}	0.50 mS	C_3	275 pF
C_{00}	500 pF	C_{11}	500 pF

Table 2. Coupling factors of the analyzed example.

Desired Couplings	Value	Undesired Couplings	Value
k_{01}	14.3%	k_{12}	6.2%
k_{02}	46.3%	k_{13}	16.1%
k_{03}	32.2%	k_{23}	3.5%

Electric coupling is realized by the coupled capacitors C_j ($j = 0, 1, 2, 3$). In each transmitter and in the receiver, a resonant circuit is constructed by adding a shunt inductor L_j with value

$$L_j = \frac{1}{\omega_0^2 C_j}. \tag{58}$$

The corresponding values are given in Table 3.

In order to verify the analytical formulas, the numerical example has been simulated in AWR NI. Figure 3b depicts the applied equivalent circuit for the simulation of the capacitive coupling [25].

First of all, the admittance matrix of the link has been calculated, obtaining the following values:

$$Y = \begin{bmatrix} 1 + 31.42\,j & -1.26\,j & -3.14\,j & -3.14j \\ -1.26\,j & 1.5 & -0.628\,j & -9.42\,j \\ -3.14\,j & -0.628\,j & 0.5 & -6.28\,j \\ -3.14\,j & -9.42\,j & -6.28\,j & 1 + 31.42j \end{bmatrix} \cdot 10^{-3}. \tag{59}$$

By using the values reported in Equation (59), the extended kQ-product α_n, the system kQ-product α_N, and the inductors L_j, can be calculated from Equations (28), (27), and (58), respectively, and are listed in Table 3.

Table 3. Calculated network simulation parameters for the example capacitive power transfer (CPT) system.

Quantity	Value	Quantity	Value
L_0	724 nH	α_1	3.1
L_1	724 nH	α_2	7.7
L_2	844 nH	α_3	8.9
L_3	921 nH	α_N	12.2

As per the maximum efficiency, a value of 84.9% is attainable, according to Equation (31). The parameters at which the maximum efficiency configuration is reached are listed in Table 4. A current source I_1^S of the first transmitter of 100 mA was chosen, resulting in the optimal current sources of the other transmitters, according to Equation (47).

The optimal load admittance is calculated by Equations (55) and (56). The optimal load susceptance is negative, i.e., it corresponds to a shunt inductor $L_0^{L,opt}$.

Additionally, according to Equation (41) a shunt susceptance at each transmitter side is necessary to compensate the transmitter's cross-coupling. At the first transmitter, the shunt susceptance is an inductor L_1^S. At the second and third transmitter, it is found that the shunt susceptances are capacitors C_2^S and C_3^S. All the values calculated from theoretical formulas are summarized in Table 4.

Table 4. Calculated values for the maximum efficiency solution.

Quantity	Value	Quantity	Value
I_2^S	300 mA	I_3^S	200 mA
$G_0^{L,opt}$ $(R_0^{L,opt})$	12.2 mS (81.9 Ω)	L_1^S	974 nH
$L_0^{L,opt}$	506 nH	C_2^S	30.0 pF
η_{max}	84.9%	C_3^S	17.5 pF

First, the simulation is executed at the maximum-efficiency configuration of Table 4. The simulation program returns a power-transfer efficiency η of 84.9% and confirms that the output voltage V_0 is orthogonal to the input voltages and currents.

Next, the load conductance and load susceptance are varied, respectively, while keeping the other parameters fixed at their optimal value given in Table 4. The simulation results are depicted in Figures 4 and 5.
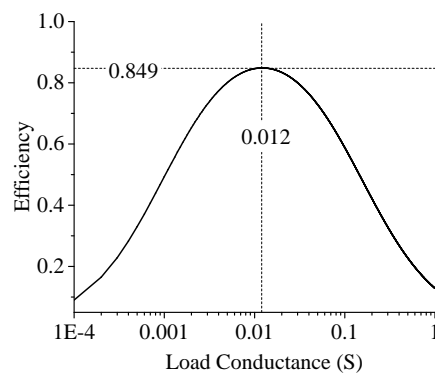

Figure 4. The simulated efficiency η as a function of varying load conductance for the given system of three transmitters and a single receiver. The load conductance is varied, while keeping the other system parameters at their optimal value.
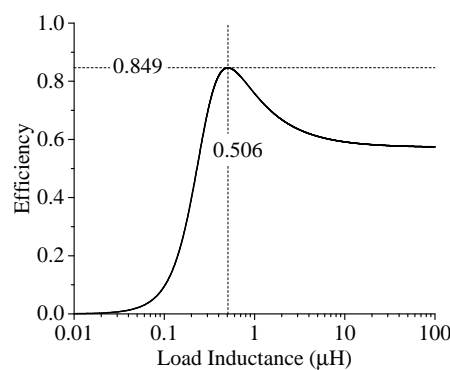

Figure 5. The simulated efficiency η as a function of varying shunt load inductance for the given system of three transmitters and a single receiver. The load inductance is varied, while keeping the other system parameters at their optimal value.

Regarding effect on the efficiency of the compensating shunt susceptances L_1^S, C_2^S, and C_3^S, this is investigated in Figures 6 and 7. The simulated efficiency confirms that maximum efficiency is obtained by using the compensating shunt susceptances calculated by using the theoretical formulas.
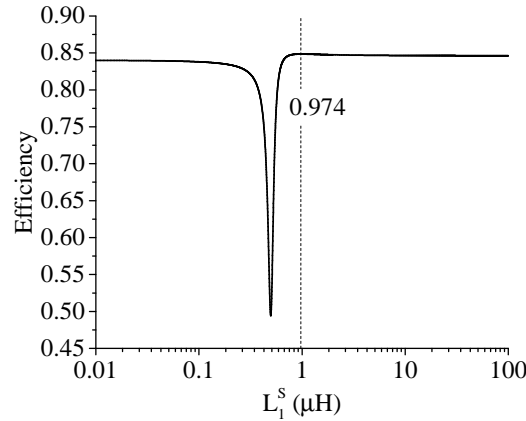

Figure 6. The simulated efficiency η as a function of the compensating susceptance L_1^S. L_1^S is varied, while keeping the other system parameters at their optimal value.

Figure 7. The simulated efficiency η as a function of the compensating susceptance C_2^S and C_3^S. C_2^S (black curve) or C_3^S (red curve) is varied, while keeping the other system parameters at their optimal value.

Additionally, the simulation confirms that the shunt susceptances at the input ports eliminate the cross-coupling. For the circuit without the compensating shunt susceptances and no cross-coupling, the same maximum efficiency of 84.9% is reached.

Finally, the effect of the amplitude of the input currents has been analyzed. The achieved results are summarized in Figure 8. It is observed that the efficiency is always lower than the optimal current distribution from Table 4 (i.e., $I_2/I_1 = 3$ and $I_3/I_1 = 2$). For example, if all input current sources are equal to 100 mA, an efficiency of 76.2% is attained.

The case of voltage sources has been also analyzed; in this case, by using Equation (57) and the values of Equation (59), the optimal voltage ratios can be determined, e.g.,

$$\frac{V_2}{V_1} = \frac{\frac{b_{02}}{g_{22}}}{\frac{b_{01}}{g_{11}}} = 2. \tag{60}$$

Analogously, the optimal ration $V_3/V_1 = 4$ is found. This is confirmed by circuital simulation results summarized in Figure 9.
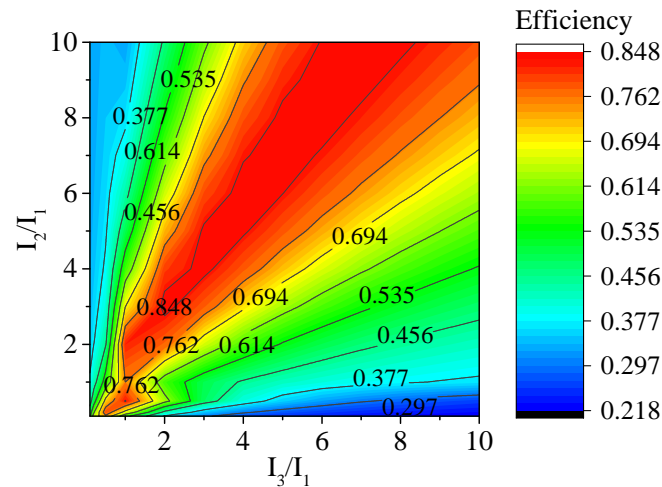

Figure 8. The simulated efficiency η as a function of the ratio of the input currents. The efficiency is always lower than the optimal current distribution $I_2/I_1 = 3$ and $I_3/I_1 = 2$. For example, if all input current sources are equal (i.e., $I_2/I_1 = 1$ and $I_3/I_1 = 1$), an efficiency of 76.2% is attained.
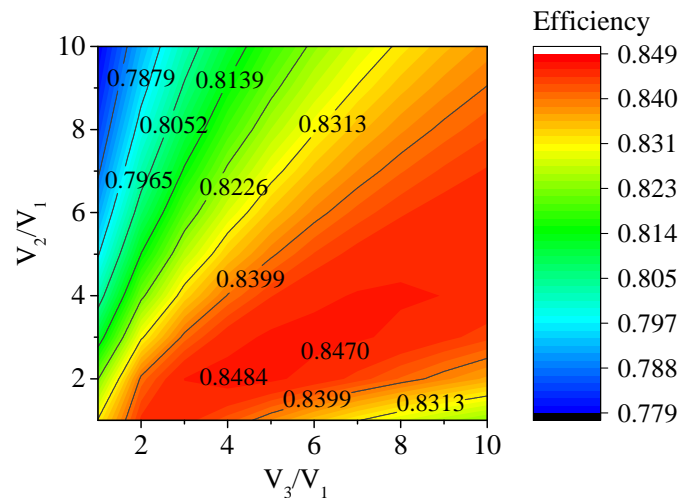

Figure 9. The simulated efficiency η as a function of the ratio of the input voltages.

In conclusion, circuital simulations confirm the data provided by the theory for the analyzed example: a maximum power-transfer efficiency is achieved for the optimal values of Table 4, calculated according to analytical derivation.

7. Conclusions

A general CPT system with any number of transmitters and a single receiver was optimized towards power-transfer efficiency. It was shown that in order to maximize the efficiency of a system with given wireless links and couplings, three conditions must be fulfilled simultaneously. First, the ratio of the input current sources is dependent on the coupling between each transmitter and the receiver, given by Equation (47). Secondly, the undesired cross-coupling between the transmitters themselves can be eliminated by adding appropriate shunt susceptances, given by Equation (41), at the input terminals. Finally, the optimal load is purely resistive, equal to Equation (55), if the receiver

has no self-susceptance. If a self-susceptance is present at the receiver's side, a compensating load susceptance is required.

Additionally, by conjugate-matching the internal shunt admittance of the generators, the maximum-efficiency solution coincides with the configuration that maximizes the output power.

It was shown that the maximum achievable efficiency η_{max}, the optimal loads, and the optimal input currents are independent on the cross-coupling between the transmitters, since this unwanted cross-coupling can be entirely annihilated with the transmitter shunt susceptances B_n^S. As a result, it is possible to increase the system efficiency by adding more transmitters, and compensating every time for transmitter cross-coupling.

The expression for the extended kQ-factor for each transmitter–receiver link was determined, allowing an estimate of the maximum efficiency of the CPT system via the system kQ-product.

Finally, the analytical derivation was verified by simulation of an example CPT system with three transmitters and a single receiver. Measurements on a CPT setup with multiple transmitters are required to confirm the accuracy of the analytical results and are part of future research.

Author Contributions: Conceptualization, methodology, B.M., M.M.; validation, B.M., G.M., M.M.; writing–original draft preparation, B.M.; writing–review and editing, A.C., G.M., M.M. All authors have read and agreed to the published version of the manuscript.

Conflicts of Interest: The authors declare no conflict of interest.

References

1. Zhu, Q.; Zang, S.; Zou, L.J.; Zhang, G.; Su, M.; Hu, A.P. Study of coupling configurations of capacitive power transfer system with four metal plates. *Wireless Power Transfer* **2019**, *6*, 97–112. [CrossRef]

2. Wang, K.; Sanders, S. Contactless USB—A capacitive power and bidirectional data transfer system. In Proceedings of the IEEE Applied Power Electronics Conference and Exposition-APEC, Fort Worth, TX, USA, 16–20 March 2014; pp. 1342–1347.

3. Hu, A.P.; Liu, C.; Li, H.L. A novel contactless battery charging system for soccer playing robot. In Proceedings of the IEEE 15th International Conference on Mechatronics and Machine Vision in Practice, Auckland, New Zealand, 2–4 December 2008; pp. 646–650.

4. Culurciello, E.; Andreou, A.G. Capacitive inter-chip data and power transfer for 3-D VLSI. *IEEE Trans. Circ. Syst. II Express Briefs* **2006**, *53*, 1348–1352. [CrossRef]

5. Mostafa, T.M.; Muharam, A.; Hattori, R. Wireless battery charging system for drones via capacitive power transfer. In Proceedings of the IEEE PELS Workshop on Emerging Technologies: Wireless Power Transfer (WoW), Chongqing, China, 20–22 May 2017; pp. 1–6.

6. Sodagar, A.M.; Amiri, P. Capacitive coupling for power and data telemetry to implantable biomedical microsystems. In Proceedings of the IEEE 4th International IEEE/EMBS Conference on Neural Engineering, Antalya, Turkey, 29 April–2 May 2009; pp. 411–414.

7. Jegadeesan, R.; Agarwal, K.; Guo, Y.X.; Yen, S.C.; Thakor, N.V. Wireless power delivery to flexible subcutaneous implants using capacitive coupling. *IEEE Trans. Microwave Theory Tech.* **2016**, *65*, 280–292. [CrossRef]

8. Ramos, I.; Afridi, K.; Estrada, J.A.; Popović, Z. Near-field capacitive wireless power transfer array with external field cancellation. In Proceedings of the IEEE Wireless Power Transfer Conference (WPTC), Aveiro, Portugal, 5–6 May 2016; pp. 1–4.

9. Miyazaki, M.; Abe, S.; Suzuki, Y.; Sakai, N.; Ohira, T.; Sugino, M. Sandwiched parallel plate capacitive coupler for wireless power transfer tolerant of electrode displacement. In Proceedings of the IEEE MTT-S International Conference on Microwaves for Intelligent Mobility (ICMIM), Nagoya, Japan, 19–21 March 2017; pp. 29–32.

10. Dai, J.; Ludois, D.C. Wireless electric vehicle charging via capacitive power transfer through a conformal bumper. In IEEE Applied Power Electronics Conference and Exposition (APEC), Charlotte, NC, USA, 15 March 2015; pp. 3307–3313.

11. Sakai, N.; Itokazu, D.; Suzuki, Y.; Sakihara, S.; Ohira, T. One-kilowatt capacitive Power Transfer via wheels of a compact Electric Vehicle. In Proceedings of the IEEE Wireless Power Transfer Conference (WPTC), Aveiro, Portugal, 5–6 May 2016; pp. 1–3.

12. Sinha, S.; Kumar, A.; Regensburger, B.; Afridi, K.K. A new design approach to mitigating the effect of parasitics in capacitive wireless power transfer systems for electric vehicle charging. *IEEE Trans. Transport. Electr.* **2019**, 1040–1059. [CrossRef]

13. Monti, G.; Che, W.; Wang, Q.; Costanzo, A.; Dionigi, M.; Mastri, F.; Mongiardo, M.; Perfetti, R.; Tarricone, L.; Chang, Y. Wireless power transfer with three-ports networks: Optimal analytical solutions. *IEEE Trans. Circ. Syst. I Regul. Pap.* **2016**, *64*, 494–503. [CrossRef]

14. Ujihara, T.; Duong, Q.T.; Okada, M. kQ-product analysis of inductive power transfer system with two transmitters and two receivers. In Proceedings of the IEEE Wireless Power Transfer Conference, Taipei, Taiwan, 10–12 May 2017.

15. Duong, Q.T.; Okada, M. kQ-product formula for multiple-transmitter inductive power transfer system. *IEICE Electron. Express* **2017**, *14*, 20161167. [CrossRef]

16. Arakawa, T.; Goguri, S.; Krogmeier, J.V.; Kruger, A.; Love, D.J.; Mudumbai, R.; Swabey, M.A. Optimizing wireless power transfer from multiple transmit coils. *IEEE Access.* **2018**, *6*, 23828–23838. [CrossRef]

17. Lang, H.D.; Sarris, C.D. Semidefinite relaxation-based optimization of multiple-input wireless power transfer systems. *IEEE Trans. Microwave Theory Tech.* **2017**, *65*, 4294–4306. [CrossRef]

18. Lang, H.D.; Ludwig, A.; Sarris, C.D. Convex optimization of wireless power transfer systems with multiple transmitters. *IEEE Trans. Antennas Propagat.* **2014**, *62*, 4623–4636. [CrossRef]

19. Monti, G.; Wang, Q.; Che, W.; Costanzo, A.; Mastri, F.; Mongiardo, M. Maximum wireless power transfer for multiple transmitters and receivers. In Proceedings of the IEEE MTT-S International Conference on Numerical Electromagnetic and Multiphysics Modeling and Optimization (NEMO), Beijing, China, 27–29 July 2016; pp. 1–3.

20. Duong, Q.T.; Okada, M. Maximum efficiency formulation for inductive power transfer with multiple receivers. *IEICE Electron. Express* **2016**, *13*, 20160915–20160915. [CrossRef]

21. Yoon, I.J.; Ling, H. Investigation of near-field wireless power transfer under multiple transmitters. *IEEE Antennas Wirel. Propag. Lett.* **2011**, *10*, 662–665. [CrossRef]

22. Minnaert, B.; Stevens, N. Optimal analytical solution for a capacitive wireless power transfer system with one transmitter and two receivers. *Energies* **2017**, *10*, 1444. [CrossRef]

23. Minnaert, B.; Mongiardo, M.; Costanzo, A.; Mastri, F. Maximum Efficiency Solution for Capacitive Wireless Power Transfer with N Receivers. *Wireless Power Transfer* **2020**, 1–11. [CrossRef]

24. Huang, L.; Hu, A.P. Defining the mutual coupling of capacitive power transfer for wireless power transfer. *Electron. Lett.* **2015**, *51*, 1806–1807. [CrossRef]

25. Hong, J.S.G.; Lancaster, M.J. *Microstrip Filters for RF/Microwave Applications*, 1st ed.; John Wiley & Sons: New York, NY, USA, 2001; pp. 235–253.

26. Boyd, S.; Vandenberghe, L. *Convex Optimization*, 2nd ed.; Cambridge University Press: Cambridge, UK, 2004; pp. 140.

27. Ohira T. Extended k-Q product formulas for capacitive-and inductive-coupling wireless power transfer schemes. *IEICE Electron. Express* **2014**, *11*, 20140147. [CrossRef]

28. Minnaert, B.; Stevens, N. Single variable expressions for the efficiency of a reciprocal power transfer system. *Int. J. Circ. Theory Appl.* **2017**, *10*, 1418–1430. [CrossRef]

29. Sugiyama, R.; Duong, Q.T.; Okada, M. kQ-product analysis of multiple-receiver inductive power transfer with cross-coupling. In Proceedings ot the International Workshop on Antenna Technology: Small Antennas, Innovative Structures, and Applications (iWAT), Athens, Greece, 1–3 March 2017.

30. Dionigi, M.; Mongiardo, M.; Monti, G.; Perfetti, R. Modelling of wireless power transfer links based on capacitive coupling. *Int. J. Numer. Model. Electron. Netw. Dev. Fields* **2017**, *30*, e2187. [CrossRef]

31. Kracek, J.; Svanda, M. Analysis of Capacitive Wireless Power Transfer. *IEEE Access.* **2018**, *7*, 26678–26683. [CrossRef]

32. Kim, D.H.; Ahn, D. Optimization of Capacitive Wireless Power Transfer System for Maximum Efficiency. *J. Electr. Eng. Technol.* **2020**, *15*, 343–352. [CrossRef]